RSC Advances

ROYAL SOCIETY OF CHEMISTRY

www.rsc.org/advances

Journal Name

RSCPublishing

ARTICLE

$Ba_7(BO_3)_3GeO_4X$ (X=Cl, Br): the borogermanate halides with rigid GeO_4 tetrahedra and flexible XBa_6 octahedra

Cite this: DOI: 10.1039/xoxxoooooox

Received ooth January 2012,
Accepted ooth January 2012

DOI: 10.1039/xoxxoooooox

www.rsc.org/

Ming Wen,[ab] Zhipeng Lian,[c] Hongping Wu,[*a] Xin Su,[ab] Qingfeng Yan,[c] Juanjuan Lu,[ab] Zhihua Yang[*a] and Shilie Pan[*a]

The first borogermanate halides, $Ba_7(BO_3)_3GeO_4X$ (X=Cl, Br) have been synthesized by high temperature solution method. $Ba_7(BO_3)_3GeO_4X$ (X=Cl, Br) are isostructural and crystallize in the orthorhombic space group *Pbam* (no. 55). They feature a Ba−based 3D framework, while isolated GeO_4 tetrahedra and BO_3 triangles are filled in the space created by the framework. Significantly, $Ba_7(BO_3)_3GeO_4X$ (X=Cl, Br) possess similar formula with the borosilicate halides, $Ba_7(BO_3)_3SiO_4X$ (X=Cl, Br), while they are not isostructural. A interpretation for the structural transformation between them is demonstrated here considering rigid GeO_4 tetrahedra and flexible XBa_6 (X=Cl, Br) octahedra. IR spectrum, UV-Vis-NIR diffuse reflectance spectrum and first-principles calculations have been carried out on title compounds.

Introduction

Borates have been widely investigated owing to their rich chemistry structures.[1-9] Especially the borates with planar BO_3 units have attracted considerable attention, because the π-delocalization of BO_3 group is beneficial for strong second-harmonic generation (SHG) response and large birefringence based on anionic group theory. A statistical analysis of borate fundamental building blocks, carried out by P. Becker,[10] indicates that the borates with isolated BO_3 groups will be found in the system with appropriate cations/boron ratios (>1). Thus, in the alkaline-earth borates the formula $M_7(BO_3)_3F_5$ (M=Ba or Sr) with a large cations/boron ratio have attracted scientist's interests.

In the $M_7(BO_3)_3F_5$ (M=Ba or Sr) system, two compounds $Ba_7(BO_3)_3F_5$[11] and $Ba_3Sr_4(BO_3)_3F_5$[11] were first identified by Keszler *et al* in 1994. In 2008, Zhang's group has reinvestigated the crystal structure of $Ba_3Sr_4(BO_3)_3F_5$ and grown large crystal by the top-seeded solution growth method, which shows an SHG intensity about 0.5 times as large as that of KH_2PO_4 (KDP).[12] Then in 2012, Bekker *et al* has systematically studied the $M_7(BO_3)_3F_5$ (M=Ba or Sr) system. They found that the system exists disorders between $(4F)^{4-}$ and $(BO_3F)^{4-}$ and a series compounds of $Ba_7(BO_3)_{4-x}F_{2+3x}$ and $Ba_{4-x}Sr_{3+x}(BO_3)_{4-y}F_{2+3y}$[13-14] have been identified. However, in the crystal structure, the existence of disorder in the crystal is not favorable for the excellent physical or chemistry properties.

The basic structural units SiO_4 have been introduced into borate to replace the $(4F)^{4-}$ or $(BO_3F)^{4-}$ owing to SiO_4 tetrahedra possessing the same charge with $(4F)^{4-}$ or $(BO_3F)^{4-}$, which may solve the disorders in the crystal structure and improve the properties. Inspired by this, the compounds $Ba_7(BO_3)_3SiO_4X$ (X=Cl, Br)[15] have been synthesized by our group, in which the structural disorder disappears. $Ba_7(BO_3)_3SiO_4X$ (X=Cl, Br) have SHG response as strong as that of KDP. However, as is known to all, high reaction temperature and high viscosity of the silicate are not conducive for the growth of crystals. Comparing to silicates, germanates have lower reaction temperature. And in previous research, many alkaline and alkaline-earth metal borogermanates have been reported.[16-20] In addition, the Ge and Si elements are in the same main group and possess similar coordination environment. Guided by these ideas, the first borogermanate halides, $Ba_7(BO_3)_3GeO_4X$ (X=Cl, Br) have been successfully synthesized. Owing to the large cations/boron ratio (7:3), the BO_3 triangles and GeO_4 tetrahedra are all isolated, which is quite rare in inorganic borogermanates.[21] It is worth noted that although the Ge and Si atoms possess similarity, $Ba_7(BO_3)_3GeO_4X$ (X=Cl, Br) and $Ba_7(BO_3)_3SiO_4X$ (X=Cl, Br) crystallize in different space groups, centrosymmetric *Pbam* (no. 55) and polar $P6_3mc$ (no. 186), respectively.

Thus, we have investigated the substitution of Ge for Si in other reported borates determined by single crystal X-ray diffraction structure.[17-18, 22-28] We found that most of the compounds are isostructural (Table S1 in the Supporting Information). In these borates,[17-18, 22-28] we define a parameter of R (O/M, M=Si or Ge), which represents the mole ratio of the

O element and the substitution element. In general, a higher value of R means a lower mole ratio of the substituted element in the compounds, which causes smaller change from the substitution and more likely results in the isostructural substitution. Therefore when R is higher than 3, all the compounds are isostructural.[17,23-28] It is unusual that $Ba_7(BO_3)_3GeO_4X$ (X=Cl, Br) and $Ba_7(BO_3)_3SiO_4X$ (X=Cl, Br) are not isostructural with a quite high R value of 13. The structural transformation between $Ba_7(BO_3)_3GeO_4X$ (X=Cl, Br) and $Ba_7(BO_3)_3SiO_4X$ (X=Cl, Br) have been discussed in detail in the paper. We have also reported the spectrum and the first-principles calculations of the title compounds.

Experimental

Solid-State synthesis

Polycrystalline samples of $Ba_7(BO_3)_3GeO_4X$ (X=Cl, Br) were synthesized via conventional solid-state reactions. Stoichiometric mixtures of $BaCO_3$, $BaCl_2$, GeO_2, and B_2O_3 at a molar ratio 6.5:0.5:1:1.5 for $Ba_7(BO_3)_3GeO_4Cl$ and $BaCO_3$, $BaBr_2$, GeO_2, and B_2O_3 at a molar ratio 6.5:0.5:1:1.5 for $Ba_7(BO_3)_3GeO_4Br$ have been ground and packed into alumina crucibles. Raw materials were preheated at 600 °C for 14 h. The mixtures were heated to 900°C for $Ba_7(BO_3)_3GeO_4Cl$ and 950 °C for $Ba_7(BO_3)_3GeO_4Br$, then held for 4 days, and finally cooled to room temperature. During the sintering processes the samples have been ground thoroughly. The purity of the samples was confirmed by a powder X-ray diffraction (XRD), which agree well with the theoretical patterns of the compounds (Figure S1 in the Supporting Information).

Crystal growth

The single crystals of $Ba_7(BO_3)_3GeO_4X$ (X=Cl, Br) were grown from the high temperature solutions using NaCl−LiCl, NaBr−LiBr and B_2O_3 as the flux systems. The solutions were obtained in platinum crucibles by melting mixtures of $BaCO_3$, GeO_2, B_2O_3, NaCl and LiCl at a molar ratio of 7:1:2.5:2:5 for $Ba_7GeB_3O_{13}Cl$ and $BaCO_3$, GeO_2, B_2O_3, NaBr and LiBr at a molar ratio of 7:1:2.5:1:4 for $Ba_7GeB_3O_{13}Br$. The solutions were heated to 900 °C, dwell at this temperature for 10 h, then slowly cooled to 700 °C at a rate of 3 °C·h^{-1} and finally cooled down to room temperature at a rate of 10 °C·h^{-1}. The crystals of $Ba_7(BO_3)_3GeO_4X$ (X=Cl, Br) have been obtained, which were used for the single-crystal X-ray diffraction analysis.

Structure determination

The crystal structures of $Ba_7(BO_3)_3GeO_4X$ (X=Cl, Br) were collected by a Bruker SMART APEX II CCD diffractometer with monochromatic Mo Kα radiation at 293(2) K, which were futher integrated with the SAINT program.[29] The calculations were completed by programs from the SHELXTL crystallographic software package, while their structures were determined by direct methods with SHELXS-97. Final least-squares refinements are on F_o^2 with data having $F_o^2 \geqslant 2\sigma(F_o^2)$. PLATON has been used to checke for missing symmetry.[30] Crystal data and structure refinement information are shown in Table 1. And final refined atomic positions and isotropic thermal parameters are displayed in Table S2 in the Supporting Information.

Table 1 Crystal data and structure refinements for $Ba_7(BO_3)_3GeO_4Cl$ and $Ba_7(BO_3)_3GeO_4Br$.

Empirical formula	$Ba_7(BO_3)_3GeO_4Cl$	$Ba_7(BO_3)_3GeO_4Br$
Temperature	296(2) K	
Wavelength	0.71073 Å	
Crystal system	Orthorhombic	
Space group	*Pbam*	
Formula weight	1309.85	1354.31
a (Å)	20.353(18)	20.381(8)
b (Å)	7.416(6)	7.477(3)
c (Å)	11.123(10)	11.175(4)
Z, Volume (Å^3)	4, 1679(3)	4, 1702.9(11)
ρ_{Calcd} (Mg/m^3)	5.183	5.283
μ(/mm)	18.121	20.054
R(int)	0.0776	0.0651
Goodness-of-fit on F^2	1.037	1.043
Final R indices $[F_o^2>2\sigma(F_o^2)]$[a]	R1 = 0.0351, wR2 = 0.0612	R1 = 0.0315, wR2 = 0.0585
R indices (all data)[a]	R1 = 0.0545, wR2 = 0.0675	R1 = 0.0426, wR2 = 0.0630
Extinction coefficient	0.00061(4)	0.00207(7)
Largest diff. peak and hole (e·Å^{-3})	2.403 and -2.209	2.158 and -2.070

[a] $R_1 = \Sigma||F_o| - |F_c||/\Sigma|F_o|$ and $wR_2 = [\Sigma w(F_o^2 - F_c^2)^2 / \Sigma w F_o^4]^{1/2}$ for $F_o^2 > 2\sigma(F_o^2)$

Infrared and UV−vis−NIR diffuse reflectance spectroscopy

The infrared spectra with the range of 400−4000 cm^{-1} have been performed on Shimadzu IR Affinity-1 Fourier transform infrared spectrometer. UV−vis−NIR diffuse reflectance data have been performed on the Solid Spec-3700DUV spectrophotometer with a range from 190 to 2600 nm. Then Polytetrafluoroethylene is used as a standard. Finally we converted the reflectance spectra to absorbance by the function, $F(R) = (1 - R)^2/2R$. R represents the reflectance while F(R) represents the Kubelka−Munk remission function.[31]

Numerical calculation details

The electronic structure calculations were performed using a plane-wave basis set and pseudopotentials within density functional theory (DFT) implemented in the total-energy module CASTEP.[32] The exchange and correlation effects were treated by Perdew–Burke–Ernzerhof (PBE) in the generalized gradient approximation (GGA).[33-35] The interactions between the ionic cores and the electrons were described by Ultrasoft pseudopotentials. The following orbital electrons were treated as valence electrons: Ba $5s^25p^66s^25d^0$, Ge $4s^24p^2$, B $2s^22p^1$, O

$2s^22p^4$, Cl $3s^23p^5$ and Br $4s^24p^5$. The number of plane waves included in the basis were determined by a cutoff energy of 340 eV, and the numerical integration of the Brillouin zone was performed using a 4 × 4 × 3 Monkhorst–Pack scheme[36] k-point grid sampling for $Ba_7(BO_3)_3GeO_4Cl$ and $Ba_7(BO_3)_3GeO_4Br$. Our test showed that these computational parameters ensure a good convergence in the present studies.

The linear optical response properties of the $Ba_7(BO_3)_3GeO_4X$ (X=Cl, Br) were examined through calculating the complex dielectric function $\varepsilon(\omega) = \varepsilon_1(\omega) + i\varepsilon_2(\omega)$. The imaginary part of the dielectric function ε_2 is given in the following equation:[37]

$$\varepsilon_2\left(q \to O_{\hat{u}}, h\omega\right) = \frac{2e^2\pi}{\Omega\varepsilon_o}\sum_{kcv}\left|\left\langle\varphi_k^c\left|u\cdot r\right|\varphi_k^v\right\rangle\right|^2\delta\left[E_k^c - E_k^v - E\right]$$

The real part $\varepsilon_1(\omega)$ can be obtained from the imaginary part $\varepsilon_2(\omega)$ by the Kramers–Kronig transformation. All the other optical constants, such as the absorption spectrum, refractive index, and reflectivity are derived from $\varepsilon_1(\omega)$ and $\varepsilon_2(\omega)$.

Results and discussion

Structure

Both of the title compounds crystallize in an orthorhombic space group, *Pbam* (no. 55). As $Ba_7(BO_3)_3GeO_4X$ (X=Cl, Br) are isostructural, only the structure of $Ba_7(BO_3)_3GeO_4Br$ is described in detail here. There are six unique Ba sites, two unique B sites, one unique Ge site, one unique Br site and eight unique O sites in the asymmetric unit (Table S2 in the Supporting Information). In the structure of $Ba_7(BO_3)_3GeO_4Br$, BaO_n (n=8, 9) and BaO_7Br_2 polyhedra are interconnected by shared oxygen atoms to form the 3D framework (Figure 1a), while isolated GeO_4 tetrahedra and BO_3 triangles are filled in the space created by the framework. (Figure 1b).

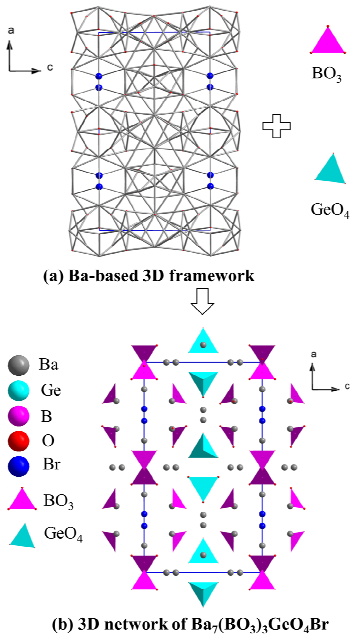

Figure 1 The structure of $Ba_7(BO_3)_3GeO_4Br$. (a) Ba−based 3D framework. (b) 3D network of $Ba_7(BO_3)_3GeO_4Br$. All the Ba−O and Ba−Br bonds have been omitted for clarity.

Selected bond distances and angles for $Ba_7(BO_3)_3GeO_4X$ (X=Cl, Br) are presented in Figure S3 in the Supporting Information. The Ba−O, B−O, Ge−O and Ba-Br distances varying over 2.567(7)−3.217(5) Å, 1.362(12)−1.391(9) Å, 1.737(7)−1.766(5) Å and 3.1424(15)−3.7463(13) Å, respectively. These values are observed in other reported compounds.[16a, 38]

Comparing the structure of $Ba_7(BO_3)_3GeO_4X$ (X=Cl, Br) with $Ba_7(BO_3)_3SiO_4X$ (X=Cl, Br).

$Ba_7(BO_3)_3SiO_4X$ (X=Cl, Br) are isostructural and crystallize in the hexagonal $P6_3mc$ space group, while $Ba_7(BO_3)_3GeO_4X$ (X=Cl, Br) crystallize in orthorhombic *Pbam*. Three unique Ba atoms, one unique B atom, one unique Si atom, four unique O atoms and one unique Br atom are in the asymmetric unit of $Ba_7(BO_3)_3SiO_4Br$. The structure of $Ba_7(BO_3)_3SiO_4Br$ are composed of a 3D Ba(3)-based framework with tunnels viewing along *c* axis, in which the $BrBa(2)_3$ chains are resided (Figure 2a). In addition, $_\infty^1[Ba(1)O_6(SiO_4)]$ single chains and isolate BO_3 triangles are filled in the framework to form its 3D network structure (Figures 2b and 2c). In the structure, the $_\infty^1[Ba(1)O_6(SiO_4)]$ single chain consists of isolated SiO_4 tetrahedra and $Ba(1)O_{10}$ polyhedra.

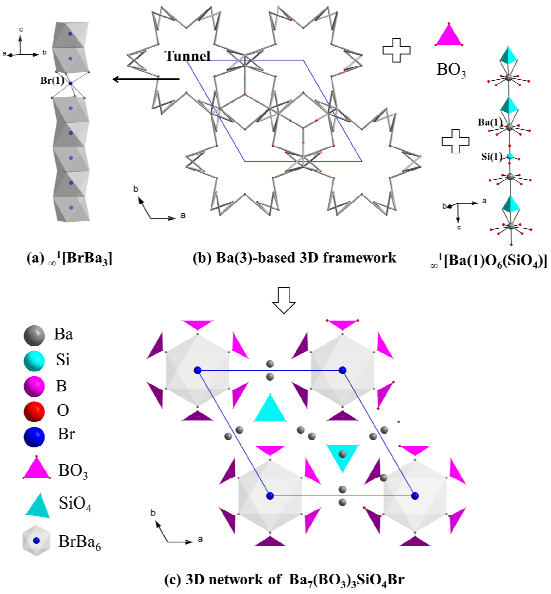

Figure 2 The structure of $Ba_7(BO_3)_3SiO_4Br$. (a) $_\infty^1[BrBa_3]$. (b) Ba(3)−based 3D framework. (c) 3D network of $Ba_7(BO_3)_3SiO_4Br$. All the Ba−O bonds have been omitted for clarity.

Similarly, the structure of $Ba_7(BO_3)_3GeO_4Br$ composes of a 3D Ba(1, 4, 5)-based framework with tunnels viewing along *b* axis, in which the $BrBa(2, 6)_3$ chains are located (Figure 2a). In

addition, $_{\infty}^{1}\{[Ba(3)O_4(GeO_4)]_2\}$ double chains and isolate BO_3 triangles are filled in the framework to form its 3D network structure (Figures 2b and 2c). The $_{\infty}^{1}\{[Ba(3)O_4(GeO_4)]_2\}$ double chain are built of isolated GeO_4 tetrahedra and $Ba(3)O_{10}$ polyhedra.

Accordingly, the structural transformation between $Ba_7(BO_3)_3SiO_4Br$ and $Ba_7(BO_3)_3GeO_4Br$ will be discussed from the following two parts: (**A**) the arrangements of chains and (**B**) the Ba-based 3D frameworks.

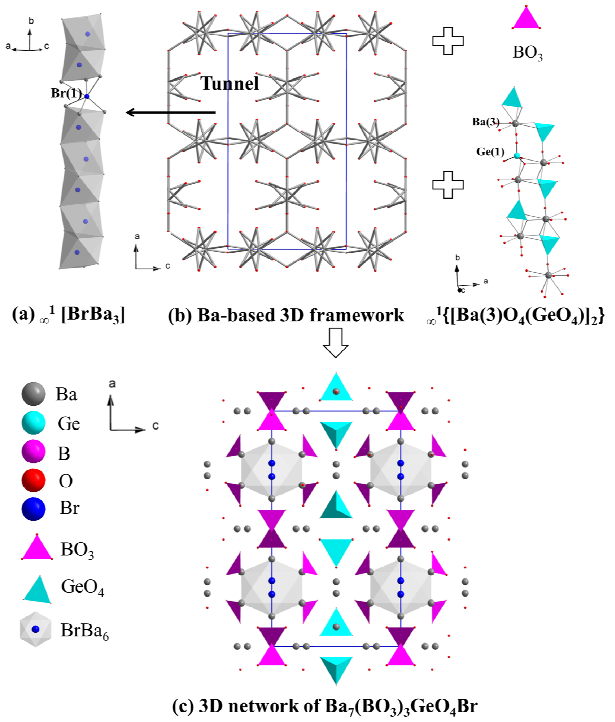

Figure 3 The structure of $Ba_7(BO_3)_3GeO_4Br$. (a) $_{\infty}^{1}$ [$BrBa_3$]. (b) Ba−based 3D framework. (c) 3D network of $Ba_7(BO_3)_3GeO_4Br$. All the Ba−O bonds have been omitted for clarity.

(A) The transformation from $_{\infty}^{1}$[Ba(1)O$_6$(SiO$_4$)] single chains to $_{\infty}^{1}${[Ba(3)O$_4$(GeO$_4$)]$_2$} double chains. In the structure of $Ba_7(BO_3)_3SiO_4Br$, the parallel single chains of $_{\infty}^{1}$[$Ba(1)O_6(SiO_4)$] are linked by $Ba(3)O_9$ polyhedra (Figure 4a). When the Si atoms are replaced by the Ge atoms, it causes a weak squeeze between GeO_4 tetrahedra and $Ba(3)O_9$ polyhedra owing to the dimensional effect (the average bond lengths of Si−O is 0.155 Å smaller than that of Ge−O). In addition, as we know, the rigid units are hard to be compressed and squeezed while the flexible ones are easy. In the structure, the SiO_4 and GeO_4 tetrahedra can be regarded as rigid due to their small bond distance variations comparing to that of Ba−O polyhedra. However, comparing with Ba−O polyhedra, the $BrBa_6$ octahedra can be regarded as flexible units for their largest bond distance variations in the structures. Thus, the $Ba(3)O_9$ polyhedra are squeezed by the rigid GeO_4 tetrahedra to the flexible $BrBa_6$ octahedra (Figure 4b). As a result, the $Ba(3)O_9$ polyhedra have been squeezed out of the chains, which leads to the single chains connect each other to form the double chains (Figures 4c and 4d).

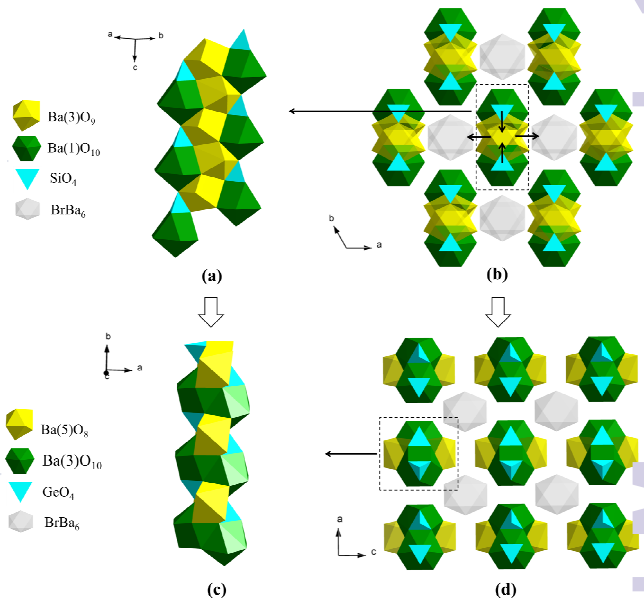

Figure 4 The transformation from $_{\infty}^{1}$[$Ba(1)O_6(SiO_4)$] single chains to $_{\infty}^{1}${[$Ba(3)O_4(GeO_4)$]$_2$} double chains. (a) $_{\infty}^{1}$[$Ba(1)O_6(SiO_4)$] single chains. (b) the arrangement of single chains and $BrBa_6$ octahedra in $Ba_7(BO_3)_3SiO_4Br$. (c) $_{\infty}^{1}${[$Ba(3)O_4(GeO_4)$]$_2$} double chains. (d) the arrangement of single chains and $BrBa_6$ octahedra in $Ba_7(BO_3)_3GeO_4Br$.

(B)The transformation of the Ba-based 3D frameworks. Both $Ba_7(BO_3)_3SiO_4Br$ and $Ba_7(BO_3)_3GeO_4Br$ have a Ba:Si or Ba:Ge molar ratio of 7:1, but the Ba atoms are arranged in different configurations. In the structure of $Ba_7(BO_3)_3SiO_4Br$, the $BrBa_6$ octahedra are in the center of neighboring six Si tetrahedra and the SiO_4 tetrahedra connect with the Ba(3) atoms to form a single chain viewing along the *c* axis (Figure 5a). From Figure 5b, we can also observe that every six Ba atoms are lied around one SiO_4 tetrahedron. The rigid SiO_4 tetrahedra have pushed the Ba(2) atoms to the Br atoms, which makes the six Ba atoms like a pattern of equilateral triangle (Figure 5b). Six equilateral triangles constitute a hexagon configuration template. These suggest that $Ba_7(BO_3)_3SiO_4Br$ crystallizes in the hexagonal crystal system. While in the structure of $Ba_7(BO_3)_3GeO_4Br$, similarly, the $BrBa_6$ octahedra are located at the center of the SiO_4 tetrahedra and the Ba atoms lie around the SiO_4 tetrahedra (Figures 5c and 5d). Owing to the squeeze from the SiO_4 tetrahedra to the Ba(2) and Ba(6) atoms, the Ba atoms form an analogous pattern of rectangle. And four rectangles compose a bigger one, which can become a rectangle template (Figure 5d). These imply that $Ba_7(BO_3)_3GeO_4Br$ crystallizes in the orthogonal crystal system.

Based on above analyses, rigid SiO_4 tetrahedra and flexible $BrBa_6$ octahedra play key roles in the structural transformation from hexagonal $Ba_7(BO_3)_3SiO_4Br$ to orthogonal $Ba_7(BO_3)_3GeO_4Br$.

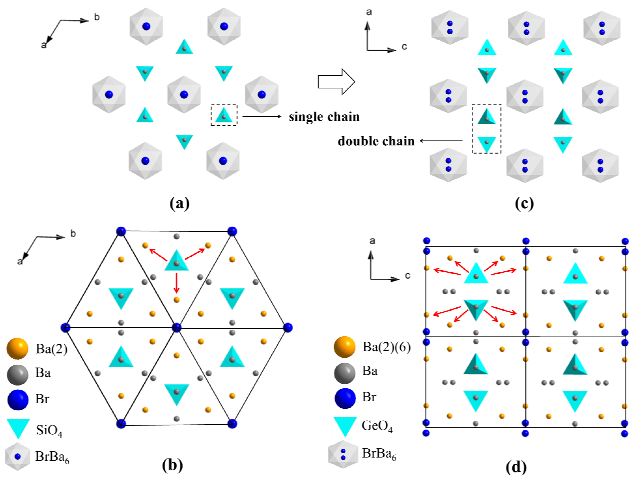

Figure 5 The comparison of different Ba-based frameworks in $Ba_7(BO_3)_3SiO_4Br$ and $Ba_7(BO_3)_3GeO_4Br$. (a) The arrangements of Si and Br atoms in $Ba_7(BO_3)_3SiO_4Br$. (b) The arrangements of Si, Ba and Br atoms in $Ba_7(BO_3)_3SiO_4Br$. (c) The arrangement of Ge and Br atoms in $Ba_7(BO_3)_3GeO_4Br$. (d) The arrangement of Ge, Ba and Br atoms in $Ba_7(BO_3)_3GeO_4Br$.

Infrared and UV-vis-NIR diffuse reflectance spectroscopy

The infrared spectroscopy of $Ba_7(BO_3)_3GeO_4X$ (X=Cl, Br) are quite same. For both of them, the bands appeared in the range of 1350−1450 cm^{-1} and 1150−1250 cm^{-1} can be assigned to the asymmetric stretching vibration of BO_3 groups (Figure S2 in the Supporting Information). The peaks observed in the region of 733−641 cm^{-1} are attributed to the out-of-bending of BO_3. The peaks in the region of 860-900 cm^{-1} can be assigned to an asymmetrical stretch of Ge−O of the tetrahedral germanium. The absorption bands in the range of 450−600 cm^{-1} correspond to the bending vibrations of the Ge−O bonds. Infrared spectra further confirm the existence of BO_3 triangles and GeO_4 tetrahedra, which is consistent with the results obtained from single crystal X-ray structural analyses.

The UV−vis−NIR diffuse reflectance spectra of $Ba_7(BO_3)_3GeO_4X$ (X=Cl, Br) are deposited in Figure S3 in the Supporting Information. It indicates that the the experimental optical band gap of $Ba_7(BO_3)_3GeO_4Cl$ and $Ba_7(BO_3)_3GeO_4Br$ are 5.28 and 5.31 eV, respectively. The large band gaps of the title compounds suggest that they may be used as the optical window materials.

Band structures, density of states and optical properties

The band structures of $Ba_7(BO_3)_3GeO_4X$ (X=Cl, Br) are presented in Figure S4 in the Supporting Information. The valence band maximum (VBM) and the conduction band minimum (CBM) are located at Γ point of the Brillouin zone indicating both of the two compounds belong to direct band-gap semiconductors. The extrapolated experimental optical gaps of 5.28 eV for $Ba_7(BO_3)_3GeO_4Cl$ and 5.31 eV for $Ba_7(BO_3)_3GeO_4Br$ are slightly larger than the calculated values 4.93 eV and 4.91 eV respectively, the underestimation of the band gap is generally due to insufficiently accuracy of exchange correlation energy under DFT methods.[39] We can see that the results of our calculation are good and give reasonable explanations for the optical absorption spectra. The highest occupied and lowest unoccupied orbitals determine the way of electronic transitions and the absorption edge. It is shown in Figure S5 in the Supporting Information that the absorption edges of $Ba_7(BO_3)_3GeO_4Cl$ and $Ba_7(BO_3)_3GeO_4Br$ are mainly decided by O 2*p* states in BO_3 units.

The total and partial densities of states (DOS and PDOS) are shown in Figure 6. The top region of VBs extends wide range from -6.7 eV to VBM. This bands mostly originate from Ge 4*s*4*p*, B 2*s*2*p* and O 2*s*2*p* states with the mixings of Ba 5*s*5*p* and Cl 3*p*/ Br 4*p* states, especially near the Fermi level. It is worthy to note that strong hybridizations occur among the Ge 4*s*4*p*, B 2*s*2*p* and O 2*s*2*p* states in the range of -6.7 eV to -0.7 eV. For $Ba_7(BO_3)_3GeO_4Cl$ and $Ba_7(BO_3)_3GeO_4Br$, the conduction bands from CBM to 8.5 eV are derived from Ba 5*d*, Ge 4*s*4*p* and B 2*p* states with mixings of Ba 5*s*5*p*, B 2*s* and O 2*s*2*p* states, implying strong interactions in Ge−O and B−O bonds for the compounds. The valence bands and conduction bands near the gap are dominated by O 2*p* and Ba 5*d* respectively. Accordingly, the absorption spectrum near the UV-Visible cut-off wavelength can be assigned as the charge transfers from O 2*p* states to the Ba 5*d* states.

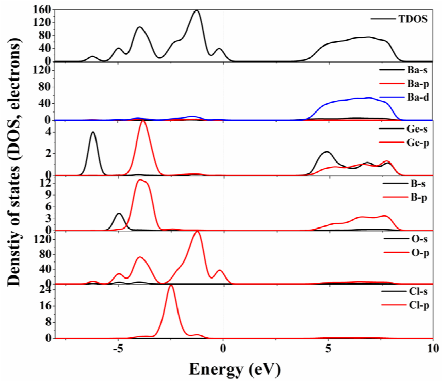

(a)

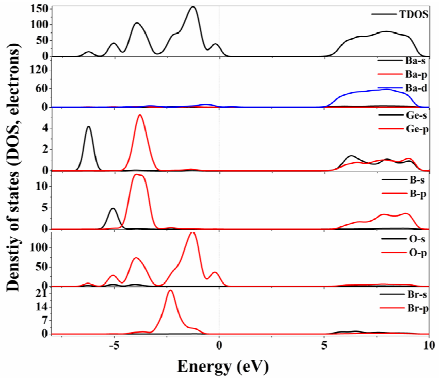

(b)

Figure 6 TDOS and PDOS plots of $Ba_7(BO_3)_3GeO_4Cl$ (a) and $Ba_7(BO_3)_3GeO_4Br$ (b).

On the basis of the electronic structures, the linear optical properties can be estimated. The imaginary part of dielectric function ε_2 is calculated, and its real part ε_1 is determined by the Kramers−Kronig transform, from which the refractive indices and the birefringence Δn were obtained.[40] The dispersion curves of refractive indices are calculated by the formula $n^2(\omega) = \varepsilon(\omega)$ displaying a similar optical anisotropy behavior: $n^x \approx n^y > n^z$ for $Ba_7(BO_3)_3GeO_4Cl$ and $Ba_7(BO_3)_3GeO_4Br$. And the birefringence (Δn) versus wavelength is shown in Figure S6 in the Supporting Information. It can be seen that the birefringences of $Ba_7(BO_3)_3GeO_4Cl$ and $Ba_7(BO_3)_3GeO_4Br$ are about 0.03 with the wavelength at 1064 nm.

Conclusion

The first borogermanate halides, $Ba_7(BO_3)_3GeO_4X$ (X=Cl, Br) have been obtained by high temperature solution method. We have discussed the structural transformation from $Ba_7(BO_3)_3SiO_4X$ (X=Cl, Br) to $Ba_7(BO_3)_3GeO_4X$ (X=Cl, Br). The unusual structural transformation mainly originates from rigid GeO_4 tetrahedra and flexible XBa_6 (X=Cl, Br) octahedra. We believe that this interpretation can give new insights into structural transformation. The first-principles calculations show that the calculated band gaps (4.93 eV for $Ba_7(BO_3)_3GeO_4Cl$ and 4.91 eV for $Ba_7(BO_3)_3GeO_4Br$) agree well with the experiment ones (5.28 and 5.31 eV). The top of the valence band is dominated by the mixture of B 2*p* and O 2*p* states, while the Ba 5*d*, Ge 4*s*4*p*, B 2*s* and O 2*s*2*p* states dominate the bottom of the conduction band.

Acknowledgements

This work was supported by the National Natural Science Foundation of China (Grant Nos. 21201176, U1303392, 51425206, 51172277, U1129301), 973 Program of China (Grant No. 2014CB648400), the Xinjiang Program of Cultivation of Young Innovative Technical Talents (Grant No. 2014711001), the Western Light of CAS (Grant No. XBBS201214), the Outstanding Young Scientists Project of Chinese Academy of Science. the Xinjiang International Science & Technology Cooperation Program (20146001), the Funds for Creative Cross & Cooperation Teams of CAS, Xinjiang Key Laboratory Foundation (Grant No. 2014KL009).

Notes and references

[a]*Key Laboratory of Functional Materials and Devices for Special Environments of CAS, Xinjiang Key Laboratory of Electronic Information Materials and Devices, Xinjiang Technical Institute of Physics & Chemistry of CAS, 40-1 South Beijing Road, Urumqi 830011, China. E-mail: wuhp@ms.xjb.ac.cn., slpan@ms.xjb.ac.cn; Fax: +(86)-991-3838957; Tel: +(86)-991-3674558*

[b]*University of Chinese Academy of Sciences, Beijing 100049, China*

[c]*Department of chemistry, Tsinghua University, Beijing, 100084, China*

† Electronic supplementary information (ESI) available: Calculated and observed XRD patterns, IR and UV-vis-NIR diffuse transmittance spectra, the substitution of Ge for Si in borates, final refined atomic positions and isotropic thermal parameters, selected bond distances and angles and first-principles calculations in $Ba_7(BO_3)_3GeO_4X$ (X=Cl, Br). CCDC 1058752 for $Ba_7(BO_3)_3GeO_4Cl$ and CCDC 1058753 for $Ba_7(BO_3)_3GeO_4Br$. For ESI and crystallographic data in CIF or other electronic format see DOI: 10.1039/x0xx00000x

1 (a) P. Becker, *Adv. Mater.*, 1998, **10**, 979. (b) C. T. Chen, B. C. Wu, A. Jiang and G. M. You, *Sci. Sin. B*, 1985, **28**, 235. (c) C. T. Chen, Y. C. Wu, A. Jiang, B. C. Wu, G. M. You, R. K. Li and S. J. Lin, *J. Opt. Soc. Am. B*, 1989, **6**, 616. (d) Y. C. Wu, T. Sasaki, S. Nakai, A. Yokotani, H. Tang and C. T. Chen, *Appl. Phys. Lett.*, 1993, **62**, 2614

2 (a) Y. Mori, I. Kuroda, S. Nakajima, T. Sasaki and S. Nakai, *Appl. Phys. Lett.*, 1995, **67**, 1818. (b) C. T. Chen, Y. B. Wang, B. C. Wu, K. C. Wu, W. L. Zeng and L. H. Yu, *Nature*, 1995, **373**, 322. (c) N. Ye, W. R. Zeng, J. Jiang, B. C. Wu, C. T. Chen, B. H. Feng and L. Zhang, *J. Opt. Soc. Am.*, 2000, **17**, 764. (d) L. Y. Li, G. B. Li, Y. X. Wang, F. H. Liao and J. H. Lin, *Chem. Mater.*, 2005, **17**, 4174.

3 (a) H. W. Huang, L. J. Liu, S. F Jin, W. J. Yao, Y. H. Zhang and C. T. Chen, *J. Am. Chem. Soc.*, 2013, **135**, 18319. (b) H. W. Huang, Y. He, Z. S. Lin, L. Kang and Y. H. Zhang, *J. Phys. Chem. C*, 2013, **117**, 22986. (c) R. H. Cong, J. L. Zhu, Y. X. Wang, T. Yang, F. H. Liao, C. Q. Jin and J. H. Lin, *CrystEngComm*, 2009, **11**, 1971.

4 (a) S. G. Zhao, P. F. Gong, S. Y. Luo, S. J. Liu, L. N. Li, M. A. Asghar, T. Khan, M. C. Hong, Z. S. Lin and J. H. Luo, *J. Am. Chem. Soc.*, 2015, **137**, 2207. (b) S. L. Pan, J. P. Smit, M. R. Marvel, E. S. Stampler, J. M. Haag, J. Baek, P. S. Halasyamanin and K. R. Poeppelmeier, *J. Solid State Chem.*, 2008, **181**, 2087. (c) T. Pilz and M. Jansen, *Z. Anorg. Allg. Chem.*, 2011, **637**, 1.

5 (a) H. P. Wu, H. W. Yu, Z. H. Yang, X. L. Hou, X. Su, S. L. Pan, K. R. Poeppelmeier and J. M. Rondinelli, *J. Am. Chem. Soc.*, 2013, **135**, 4215. (b) X. W. Zhang, H. W. Yu, H. P. Wu, S. L. Pan, A. Q. Jiao, B. B. Zhang and Z. H. Yang, *RSC Adv.*, 2014, **4**, 13195. (c) H. Y. Li, H. P. Wu, X. Su, H. W. Yu, S. L. Pan, Z. H. Yang, Y. Lu, J. Han and K. R. Poeppelmeier, *J. Mater. Chem. C*, 2014, **2**, 21704. (d) K. Wu, S. L. Pan and Z. H. Yang, *RSC Adv.*, 2015, **5**, 33646.

6 (a) C. Y. Bai, S. J. Han, S. L. Pan, B. B. Zhang, Y. Yang, L. Li, Z. H. Yang, *RSC Adv.*, 2015, **5**, 12416. (b) Y. Yang, S. L. Pan, X. Su, Y. Wang, Z. H. Yang, J. Han, M. Zhang and Z. H. Chen, *CrystEngComm*, 2014, **16**, 1978. (c) Z. Wang, Q. Jing, M. Zhang, X. Y. Dong, S. L. Pan and Z. H. Yang, *RSC Adv.,* 2014, **4**, 54194. (d) H. P. Wu, H. W. Yu, S. L. Pan, A. Q. Jiao, H. Y. Li, J. Han, K. Wu and S. J. Han, *Dalton Trans.*, 2014, **43**, 4886.

7 (a) A. H. Reshak, X. A. Chen, S. Auluck, H. Kamarudin, J. Chyský, A. Wojciechowski and I. V. Kityk, *J. Phys. Chem. B*, 2013, **117**, 14141. (b) X. A. Chen, H. Yin, X. N. Chang, H. G. Zang and W. Q. Xiao, *J. Solid State Chem.*, 2010, **183**, 2910.

8 (a) C. D. McMillen, J. T. Stritzinger and J. W. Kolis, *Inorg. Chem.*, 2012, **51**, 3953. (b) C. Heyward, C. McMillen and J. W. Kolis, *Inorg. Chem.*, 2012, **51**, 3956.

9 (a) H. Emme, M. Valldor, R. Pöttgen and H. Huppertz, *Chem. Mater.*, 2005, **17**, 2707. (b) J. S. Knyrim, H. Emme, M. Döblinger, O. Oeckler, M. Weil, and H. Huppertz, *Chem. Eur. J.*, 2008, **14**,

6149. (c) M. J. Xia, B. Xu and R. K. Li, *J. Cryst. Growth*, 2014, **404**, 65.
10 P. Becker, *Z. Kristallogr.*, 2001, **216**, 523.
11 D. A. Keszler, A. Akella, K. I. Schaffers and T. Alekel, *Mater. Res. Soc. Symp. Proc.*, 1994, **329**, 15.
12 G. C. Zhang, Z. L. Liu, J. X. Zhang, F. D. Fan, Y. C. Liu and P. Z. Fu, *Cryst. Growth & Des.*, 2009, **9**, 3139.
13 T. B. Bekker, S. V. Rashchenko, V. V. Bakakin, Y. V. Seryotkin, P. P. Fedorov, A. E. Kokha and S. Y. Stonogaa, *CrystEngComm*, 2012, **14**, 6910.
14 S. V. Rashchenko, T. B. Bekker, V. V. Bakakin, Y. V. Seryotkin, V. S. Shevchenko, A. E. Kokh and S. Y. Stonoga, Cryst. *Growth & Des.*, 2012, **12**, 2955.
15 X. X. Lin, F. F. Zhang, S. L. Pan, H. W. Yu, F. Y. Zhang, X. Y. Dong, S. J. Han, L. Y. Dong, C. Y. Bai and Z. Wang, *J. Mater. Chem. C*, 2014, **2**, 4257.
16 (a) X. Xu, C. L. Hu, F. Kong, J. H. Zhang and J. G. Mao, *Inorg. Chem.*, 2011, **50**, 8861. (b) D. B. Xiong, J. T. Zhao, H. H. Chen and X. X. Yang, Chem. Eur. J., 2007, 13, 9862.
17 (a) J. H. Zhang, F. Kong and J. G. Mao, *Inorg. Chem.*, 2011, **50**, 3037. (b) Y. C. Hao, C. L. Hu, X. Xu, F. Kong and J. G. Mao, *Inorg. Chem.*, 2013, **52**, 13644. (c) J. B. Parise and T. E. Gier, *Chem. Mater.*, 1992, **4**, 1065.
18 Z. E. Lin, J. Zhang and G. Y. Yang, *Inorg. Chem.*, 2003, **42**, 1797.
19 (a) H. X. Zhang, J. Zhang, S. T. Zheng, G. M. Wang and G. Y. Yang, *Inorg. Chem.*, 2004, **43**, 6148. (b) D. B. Xiong, H. H. Chen, M. R. Li, X. X. Yang and J. T. Zhao, *Inorg. Chem.*, 2006, **45**, 9301.
20 (a) P. Becker, *Cryst. Res. Technol.*, 2001, **2**, 119. (b) B. Petermüller, L. L. Petschnig, K. Wurst, G. Heymann and H. Huppertz, *Inorg. Chem.*, 2014, **53**, 9722.
21 B. F. Dzhurinskii, A. B. Pobedina, K. K. Palkina and M. G. Komova, *Russ. J. Inorg. Chem.*, 1998, **43**, 1488.
22 M. Ihara and F. Kamei, *J. Ceram. Soc. Jpn.*, 1980, **88**, 32.
23 H. P. Wu, H. W. Yu, S. L. Pan, Z. J. Huang, Z. H. Yang, X. Su and K. R. Poeppelmeier, *Angew. Chem. Int. Ed.*, 2013, **52**, 3406.
24 X. Xu, C. L. Hu, F. Kong, J. H. Zhang, J. G. Mao and J. L. Sun, *Inorg. Chem.*, 2013, **52**, 5831.
25 T. Berger and K. J. Range, *Z. Naturforsch. B*, 1996, **51**, 172.
26 C. Heyward, C. D. McMillen and J. J. Kolis, *Solid State Chem.*, 2013, **203**, 166.
27 V. R. Samygina, E. A. Genkina, B. A. Maksimov and N. I. Leonyuk, *Kristallografiya*, 1993, **38**, 61.
28 A. A. Kaminskii, B. V. Mill, E. L. Belokoneva and A. V. Butashin, *Izv. Akad. Nauk SSSR*, 1990, **26**, 1105.
29 SAINT, Version 7.60A; Bruker Analytical X-ray Instruments, Inc. Madison, WI, 2008.
30 A. L. Spek, *J. Appl. Cryst.*, 2003, **36**, 7.
31 (a) P. Kubelka and F. Z. Munk, *Tech. Phys.*, 1931, **12**, 593. (b) J. Tauc, *Mater. Res. Bull.*, 1970, **5**, 721.
32 S. J. Clark, M. D. Segall, C. J. Pickard, P. J. Hasnip, M. J. Probert, K. Rrfson and M. C. Payne, *Z. Kristallogr.*, 2005, **220**, 567.
33 J. P. Perdew, K. Burke and M. Ernzerhof, *Phys. Rev. Lett.*, 1996, **77**, 3865.
34 J. S. Lin, A. Qteish, M. C. Payne and V. Heine, *Phys. Rev. B.*, 1993, **47**, 4174.
35 A. M. Rappe, K. M. Rabe, E. Kaxiras and J. D. Joannopoulos, *Phys. Rev. B*, 1990, **41**, 1227.
36 H. J. Monkhorst and J. D. Pack, *Phys. Rev. B*, 1976, **13**, 5188.
37 E. D. Palik, *Handbook of Optical Constants of Solids. Orlando*: Academic Press: New York, 1985.
38 X. Y. Dong, H. P. Wu, Y. J. Shi, H. W. Yu, Z. H. Yang, B. B. Zhang Z. H. Chen, Y. Yang, Z. J. Huang, S. L. Pan and Z. X. Zhou, *Chem. Eur. J.*, 2013, **19**, 7338.
39 R. W. Godby, M. Schluter and L. J. Sham, *Phys. Rev. B*, 1987, **36**, 6497.
40 F. Wooten, *Optical Properties of Solid*, Academic, New York, 1972.